

1 *Type of the Paper (Article.)*

2 **Efficient removal of reactive blue 19 dye by co-electrospun nanofibers**

3 **Raheel Ahmed Hakro¹, Umair Ahmed Qureshi², Raja Fahad Qureshi², Rasool Bux Mahar³,**
4 **Muzamil Khatri⁴, Farooq Ahmed², Zeeshan Khatri^{2,4*}, Ick Soo Kim^{*4}**

5 ¹ ^a Institute of Environmental Engineering and Management, Mehran University of Engineering and
6 Technology, Jamshoro, Sindh, Pakistan

7 ² Centre of Excellence in Nanotechnology and Materials, Mehran Mehran University of Engineering and
8 Technology, Jamshoro, Sindh, Pakistan

9 ³ US Pakistan Centre for advance studies in water, Mehran Mehran University of Engineering and
10 Technology, Jamshoro, Sindh, Pakistan

11 ⁴ Nano Fusion Technology Research Group, Division of Frontier Fibers, Institute for Fiber Engineering (IFES),
12 Interdisciplinary Cluster for Cutting Edge Research (ICCER), Shinshu University, Tokida 3-15-1, Ueda,
13 Nagano prefecture, 386-8567, Japan

14 * Correspondence: Zeeshan Khatri, Dr.Eng.

15 Email: zeeshan.khatri@faculty.muet.edu.pk

16 * Corresponding Author: Ick Soo Kim, Dr.Eng.

17 E-mail: kim@shinshu-u.ac.jp

20 **Abstract:** The present work demonstrates the new nanofiber mats prepared through
21 co-electrospinning of two different polymers i.e. corn protein namely Zein and Nylon-6. The
22 composite nanofiber membrane was used as an effective adsorbent material for the removal of
23 toxic reactive dye i.e. Reactive Blue 19 (RB 19) from water solution. These co-electrospun nanofibers
24 had good mechanical strength compared to zein nanofibers alone. Experimental results suggested
25 that zein/nylon nanofibers have greater potential for total removal of RB19 at room temperature
26 within 10 min of contact time from aqueous solution. The maximum capacity was found to be 70
27 mg/g of nanofibers. The mechanism of RB19 removal on proposed nanofibers is mainly through
28 hydrogen bond and electrostatic means.

29 **Keywords:** Zein; nanocomposite membrane; adsorption; wastewater; RB19.

34 **1. Introduction**

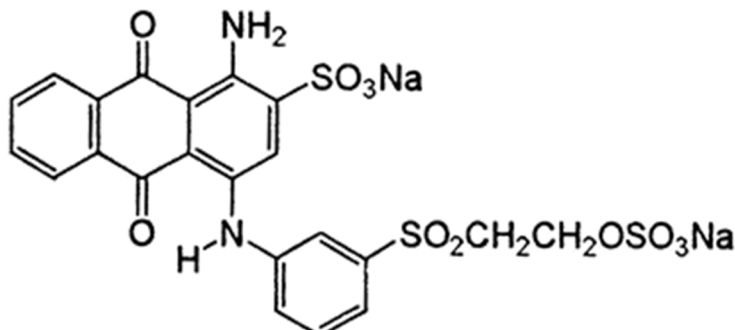
35 Industries like textile, leather, paper, rubber and many other produce large amount of wastewater
36 that is characterized by strong color content, high COD and other total suspended and dissolved
37 solids [1, 2]. The discharge of dye loaded effluent in water environment is highly undesirable for
38 both aquatic health and esthetical point of view [3]. Moreover, some of the azo dyes and their
39 metabolites are known to be potentially toxic and carcinogenic, due to their complex chemical
40 structure [4]. Therefore, the removal of such dyestuff is highly desirous. For the removal of dyes,
41 various treatment methods have been employed such as; photo-chemical degradation, advance
42 oxidation, ozonation, coagulation-flocculation and etc. [5]. Among these aforementioned methods,
43 adsorption is the most simple, low cost and highly efficient process for exclusion of various
44 pollutants including synthetic dyestuff [6]. However, the major concern in this method is selection of
45 adsorbent material with superior adsorption capacity and cheapness [7]. Previously, a wide range of
46 low cost adsorbents such as; cashew apple bagasse [8], pomegranate based activated carbon [9], rice
47 straw fly ash [10], peanut hull [11], spent tea leaves [12], etc. were utilized for the removal of reactive
48 dyes from aqueous solution. However, the adsorption capacities of these materials were low and

49 required longer pre-treatment steps [13]. In context to this, the exploration of one dimensional
50 nanoscale adsorbent especially nanofibers possess good performance due to their unique properties;
51 such as high surface to low volume ratio, highly porous morphology and better interconnectivity
52 [14]. To produce the nanofibers, one of the simple low cost methods is electrospinning in which an
53 external electric field is imposed to polymer solution to fabricate a nanofibers with a diameter of
54 submicron to nanoscale [15].

55 In recent years, the electrospinning of natural biopolymer from renewable sources such as Zein
56 has received much attention, due to its economic and environmental perspectives [16]. Zein is a
57 biological macromolecule that is biodegradable, nontoxic and biocompatible polymeric protein. It is used
58 for several applications including food packaging, drug delivery, encapsulation and etc. [17].
59 Apart from these applications zein nanofibers membrane is also reported as an adsorbent for
60 reactive dyes removal through surface modification [18]. However, the poor stability and strength of
61 zein nanofibers in aqueous medium is still a matter of concern to be fixed [19]. When zein nanofiber
62 immersed in aqueous solution, the nanofiber mates get swollen and eventually collapse into films
63 owing to distortion of interconnected pore structure [20]. One of the approach to improve the
64 properties of zein nanofiber is the blending of material that should be strong and water stable [21].
65 Therefore, in this study zein was incorporated with nylon-6 via co-electrospinning technique to
66 enhance the material strength and stability in water. The objective of this study is to explore the
67 feasibility of zein/nylon co-electrospun nanofibers as adsorbent for the removal of commonly used
68 anionic dye i.e. Reactive blue19, from aqueous solution by studying the influence of several
69 parameters including contact time, adsorbent dosage, dye concentration, and pH of solution.

70 2. Materials and Methods

71 Zein from corn (melting point 266-283°C) was purchased from Wako Pure Chemical Industries, Ltd.
72 Japan, Nylon-6(($M_w \sim 25,000$ g/mol), Formic acid (98%) purity was supplied by Sigma Aldrich. C.I
73 reactive blue 19 ($C_{22}H_{16}N_2Na_2O_{11}$) with a molecular weight (626.54 g/mol) were supplied by the
74 Sumitomo Chemical Company, Ltd., Japan. The chemical structure of the used dye is given in the
75 Fig-1.



76

77 Fig-1. Chemical structure of Reactive blue (RB19)

78 The preparation of coelectrospun nanofibers is mentioned as :

79 A solution of 60 %(wt./v) zein was prepared in DMF followed by stirring for 2 hour at room
80 temperature. Nylon-6 polymer of 22 %(wt. /v) was also prepared separately in formic acid under
81 constant stirring for 24 h at room temperature to obtain a homogeneous solution. Both these
82 solutions were loaded separately onto 5 ml plastic syringes with an inner diameter of 0.6 mm and
83 were positioned oppositely at an angle of 10° from the horizontal plane, and co-electrospinning was
84 performed simultaneously, at 20kV having tip to collector distance of 15 cm an 20 cm for both zein
85 and nylon-6 solutions, respectively, the grounded rotating metallic drum covered with aluminum

86 foil was used for the deposition of zein/nylon electrospun nanofibers. After completion of
87 co-electrospinning, the samples were dried overnight at room temperature prior to adsorption
88 experiments. The average thickness of zein/nylon nanofibers was found to be $51\pm2\mu\text{m}$.

89 The adsorption behavior of anionic dye RB19 from aqueous solution on zein/nylon
90 co-electrospun nanofiber membrane were studied at room temperature using the batch mode, the
91 experiments were performed on an automatic gallenkamp shaker by mixing a fixed adsorbent dose
92 (20 ± 0.2 mg) of nanofiber membrane in 5ml of 50mg/l of dye concentration at 200rpm, the solution
93 was shaken until the equilibrium was achieved. In order to evaluate the efficacy of dyes removal by
94 the adsorbent, following parameters were analyzed; Contact time (1-10min), pH solution (1-9),
95 adsorbent dosage (5-25mg), and initial dye concentration (50-300ppm). After the dye adsorption, the
96 nanofiber membrane were separated out manually and the samples were analyzed by Uv-vis
97 spectrophotometer for the residual dye concentration at wavelength of ($\lambda_{\text{max}}=592\text{nm}$) for RB19.

98

99 Dye removal percentage (AE %) was determined according to the following eq.

100
$$\text{Dye removal (AE \%)} = \frac{(C_0 - C_t)}{C_0} \times 100 \quad (1)$$

101 Where C_0 (mg/l) and C_t (mg/l) are the initial and final dye concentrations at time t , respectively.
102 To compare the validity of kinetic and isotherm models, error analysis was also established using
103 following relation.

104
$$\text{SSE} = \sum_{i=1}^N (q_{\text{cal}} - q_{\text{exp}})^2 \quad (2)$$

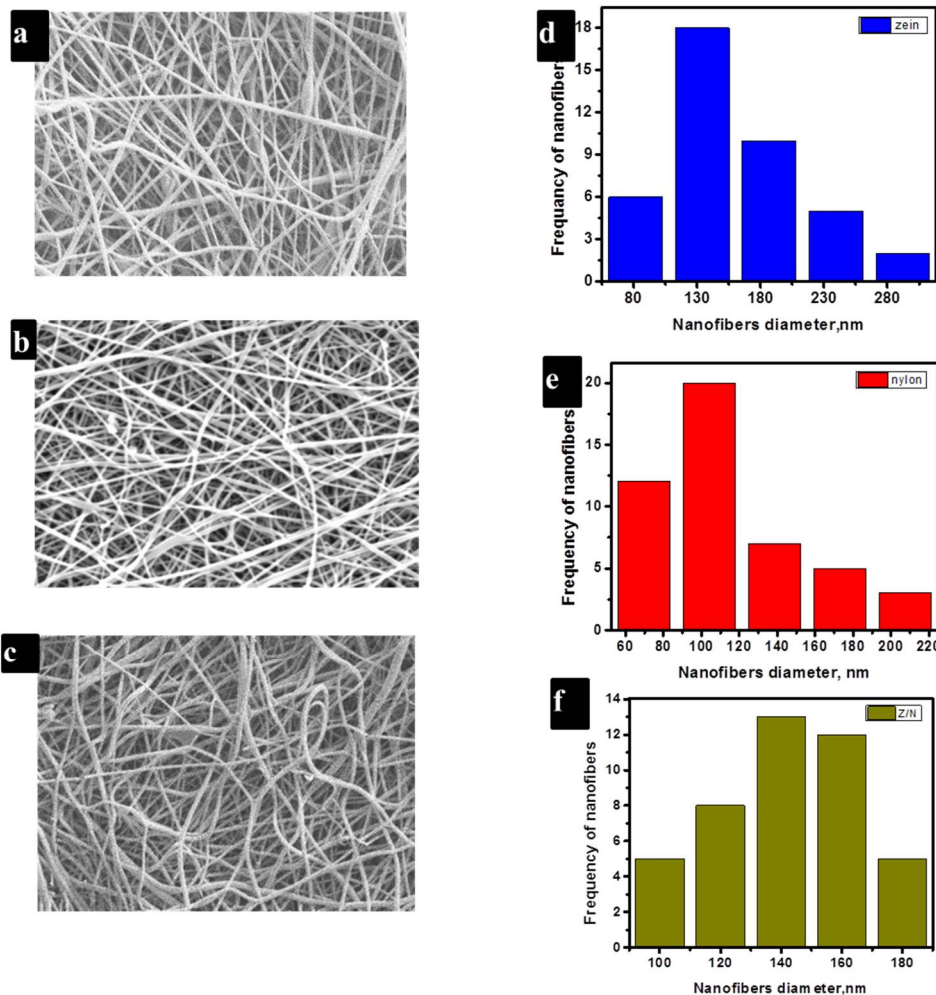
105 Where, q_{cal} and q_{exp} are the calculated and experimental adsorption capacities of zein/nylon
106 nanofibers, respectively.

107 The surface morphology of zein/nylon co-electrospun nanofibers membrane before and after
108 adsorption was examined using SEM (S3000N by Hitachi, japan) with accelerating voltage of 10kV
109 and maximum magnification of 300,000x after sputtering with Au/Pd. The average diameter of
110 nanofiber was measured using J-image analysis software (image pro R plus, version5.1, Media
111 cybernetics, Inc.) from SEM micrographs. The chemical structure of zein/nylon nanofibers
112 membrane was characterized by FTIR spectroscopy (IR presige-21 by Schimadzu, japan) using ATR
113 mode. Ultraviolet-visible (uv-vis) spectrophotometer (Perkin Elmer, USA) was used to measure
114 absorbance of dye solution before and after adsorption experiments. Tensile properties of the
115 zein/nylon nanofibers membrane was determined using titan universal tester (titan 3-910) at jog
116 speed of 1000mm/min. All the tests were performed at room temperature ($23\text{--}25\text{ }^{\circ}\text{C}$) followed by
117 ASTM D-638 Standard test method.

118 3. Results

119 3.1. Characterization

120 The SEM images of neat Zein, Nylon-6 and composite of zein/nylon nanofibers is presented in Fig-2
121 (a, b and c). The morphology of zein and nylon-6 nanofibers were bead free and smooth. The
122 average mean diameter of zein, nylon-6 and zein/nylon nanofiber were found to be 130, 100, 150 nm
123 respectively (Fig-2 d, e and f)



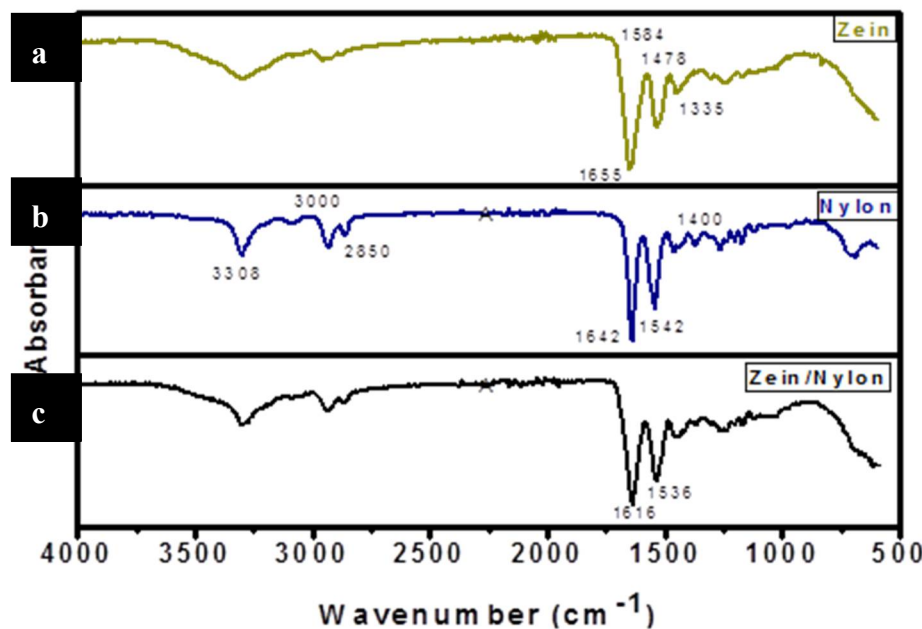
124

125 **Fig-2 (a, b, c) shows the SEM images of zein, nylon and zein/nylon nanofibers with their
126 respective diameter distribution diagram (d, e, f).**

127 The chemical analyses of neat zein, pure nylon and blended zein/nylon nanofibers were performed
128 using ATR-FTIR, in order to corroborate functional groups present in the nanofibers. The FTIR
129 spectra of nanofibers in the range of 1000-4000 cm⁻¹ are demonstrated in Fig-3. The broad absorption
130 peak at 3300 cm⁻¹ of neat zein nanofibers as shown in spectrum Fig -3(a) related to (-NH₂ stretching
131 vibration). Whereas, the characteristic bands indicative of amide vibrational bands at 1655, 1584,
132 1478 and 1335 cm⁻¹ indicated amide I, amide II, and amide III; correspond to(C=O) stretching ,(N-H)
133 bending and axial deformation vibrations of (C-N) stretching respectively [23]. On the other hand
134 spectrum (b) shows the absorption band of nylon-6. The peaks at 3308 cm⁻¹ and 2850 cm⁻¹ is mainly
135 related with NH stretching and -CH₂ symmetric stretching vibrations, respectively. The amide
136 vibrational bands at 1642cm⁻¹ (amide I, C=O stretch), and 1542 cm⁻¹ (amide II, C-N stretch and CO-
137 N-H bend). Additionally, the peak at 680 is indicative of (O-C-N) bending [24]. The peak of 1616
138 cm⁻¹ (amide I) is observed for the zein /nylon which is attributed to the amino groups of blend
139 nanofibers. The spectrum (c) of blended zein/nylon nanofibers show that the, amide I, amide II,
140 peaks were slightly shifted to lower wavenumber for zein/nylon nanofibers when compared to pure
141 zein and nylon nanofibers. For instance, the amide I peak was observed at 1616 for zein/ nylon,
142 similarly, the amide II peak was shifted to lower wavenumber as absorption peak of amide II was
143 observed at 1536, for zein/nylon. The peak shift of amide I and amide II to lower wavenumbers for
144 zein/nylon nanofibers suggested the interaction became more pronounced for nanofibers samples.
145 In fact the region from 3400-2800 of zein/nylon nanofibers resembles with nylon-6 FTIR region,

146 while the region from 1700-500 cm⁻¹ closely resemble with zein component. This confirms successful
147 blending of two different polymers.

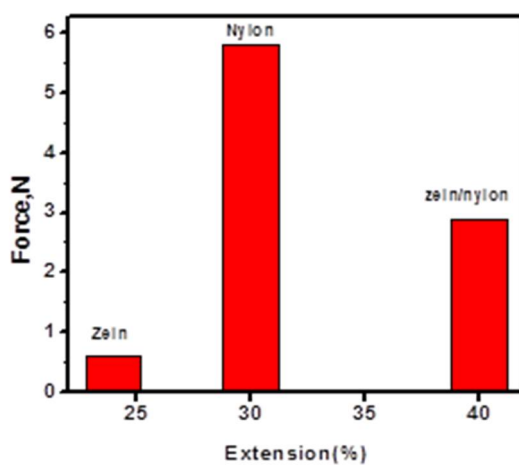
148



149

150 **Fig-3 ATR-FTIR spectra of (a) zein (b) nylon and (c) blended zein/nylon nanofibers**

151 Fig-4 shows the mechanical behavior of zein, nylon-6 and both zein/nylon-6 nanofibers. The low
152 tensile force of zein nanofibers indicate poor mechanical strength. Incorporation of nylon with zein
153 nanofibers increase the amide linkages between the zein and nylon resulting more compact
154 structure, thus slippage is reduced and elasticity improved which provide good mechanical
155 properties. Tensile strength of zein/nylon was found to be 3MPa at break of 40%.

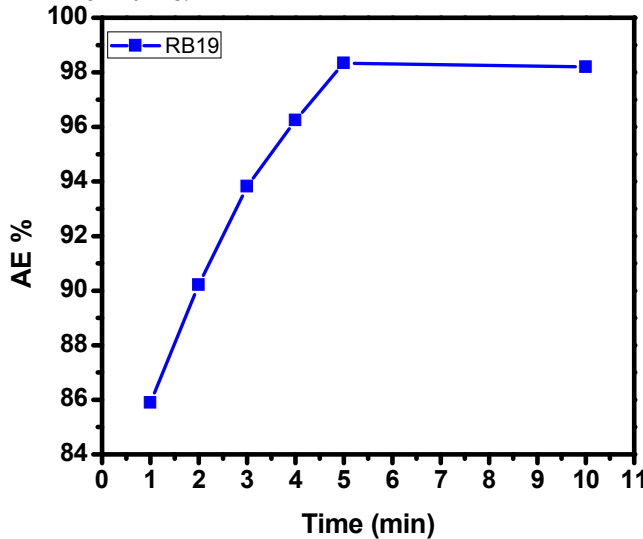


156

157 **Fig -4. Typical force-elongation performance of zein, nylon and zein/nylon-6**
158 **nanofibers**

159 3.2. *Adsorption study of nanofibers*160 3.2.1. **Effect of contact time :**

161 In order to reach to the best material for RB19 removal, it was realized to compare the
 162 adsorption efficiencies of Zein nanofiber, Nylon-6 nanofiber and Zein/Nylon-6 nanofibers. The
 163 preliminary results suggested that Zein/Nylon-6 nanofibers were comparatively better for RB19
 164 removal followed by Zein nanofibers and Nylon-6 nanofibers. Therefore, further optimization was
 165 made on composite nanofibers. Decolorization of RB19 from aqueous solution was investigated at
 166 different time intervals to attain the maximum adsorption by the zein/nylon nanofibers as presented
 167 in the Fig-5. It is clearly shown that, the rapid and significant removal of RB19 by the nanofibers
 168 membrane. was found to be 85% in just 60 seconds of contact and within 10min of shortest
 169 equilibrium time, the total dye was decolorized, which is relatively higher than other well-known
 170 adsorbents. The rapid uptake of dye is due to faster rate of dye mobility towards the abundant
 171 vacant sites of the adsorbent. After certain period of time the rate of adsorption was observed to be
 172 slightly down this trend may be due to accretion of dye molecules onto available sites [26]. This
 173 breakthrough performance of zein/nylon nanofibers is significant for industrial application due to its
 174 high efficiency at minimum time.

185 **Fig-5.** Effect of contact time on adsorption of dye

186

187 To calculate the amount of dye adsorbed, different models such as, pseudo-first-order (Eq 1),
 188 pseudo-second -order kinetic (Eq 2) and intraparticle diffusion models (Eq 3) were used [27-29].

189

190

191

192

$$\log(q_e - q_t) = \log q_e - \frac{k_1}{2.303} t \quad (1)$$

193

$$\frac{t}{q_t} = \frac{1}{k_2 q_e^2} + \frac{t}{q_e} \quad (2)$$

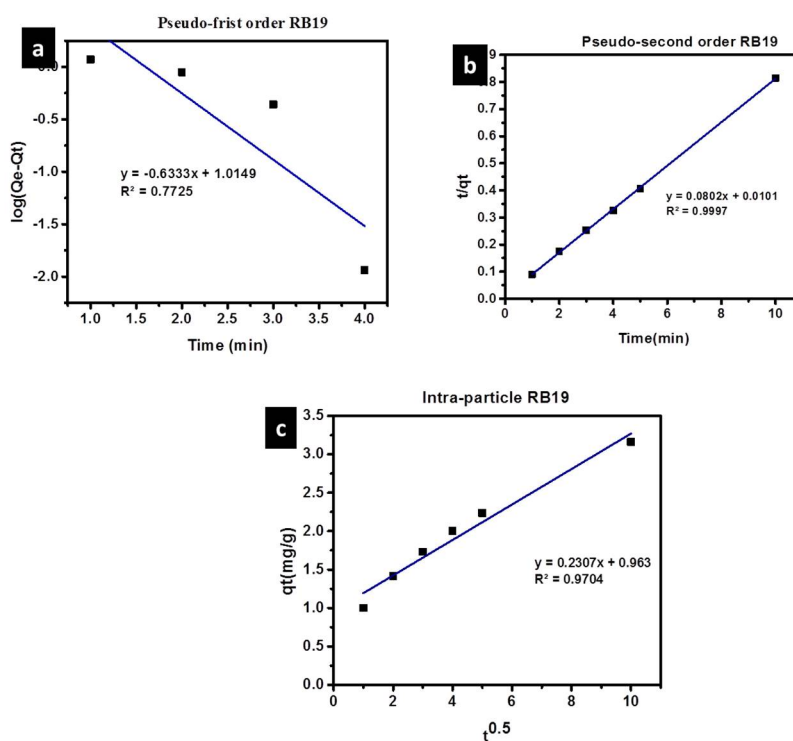
194

$$q_t = k_t t^{0.5} + c$$

195 (3)

196

197 Where q_t (mg/g) is the dye concentration on nanofibers at the time t , q_e (mg/L) is the solution
 198 phase concentration of RB19 at equilibrium. k_1 (min⁻¹), k_2 (g/mg.min) and k_i (mg/g.min^{0.5}) are the rate
 199 constants associated with pseudo first, pseudo second and intra particle diffusion models
 200 respectively. The calculated kinetics parameters and the correlation coefficients (R^2) are given in
 201 Table 1. Analysis and validation of experimental data to different models suggested that the
 202 adsorption of RB19 can be better explained by pseudo second order model rather than pseudo first
 203 order as shown in Fig-6 (a) and (b). The correlation coefficients values (R^2) for RB19 obtained from
 204 the Pseudo-second-order kinetic model were found to be over 0.99 which is greater than pseudo first
 205 order. Also the experimental values of q_e are very similar to the values calculated by the
 206 pseudo-second-order equation (q_{ecal}). Thus, the adsorption can be better described by the
 207 pseudo-second-order kinetic model rather than the pseudo-first-order kinetic model. The best fit of
 208 the second-order expression suggests that the chemisorption mechanism is involved in the
 209 adsorption [30].



210

211 **Fig-6** (a) pseudo-first (b) pseudo-second order kinetics (c) intra-particle diffusion RB19

212 To determine the rate-limiting step involved in the adsorption of dyes by the adsorbent, the
 213 intra-particle diffusion model was applied to analyze the kinetic data, according to this model the
 214 plot q_t vs $t^{0.5}$ must be linear and should pass through the origin for rate controlling mechanism in
 215 intra particle diffusion model. Fig-6(c) clearly shows that adsorption of RB19 on zein/nylon
 216 nanofiber consists linear plot between q_t vs. $t^{0.5}$ without passing through origin that does not favor
 217 intraparticle diffusion mechanism but external diffusion or surface adsorption is the rate controlling
 218 step.

219 **Table 1.** Kinetic fittings and parameters for the adsorption of RB19 on Zein/nylon-6 nanofibers

Pseudo-first order

$q_{e, exp}$ (mg/g)	$q_{e, cal}$ (mg/g)	k_1 (min ⁻¹)	R^2
12.27	10.32	1.458	0.77

Pseudo-second order

$q_{e, exp}$ (mg/g)	$q_{e, cal}$ (mg/g)	k_2 (g/mg.min)	R^2
12.27	12.46	0.632	0.99

Intraparticle Diffusion

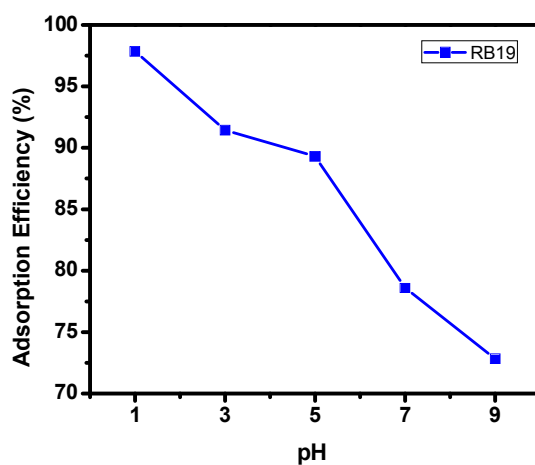
k_i (mg/g.min ^{0.5})	c	R^2
0.23	0.963	0.97

220

221 **3.2.2 The effect of pH on adsorption.**

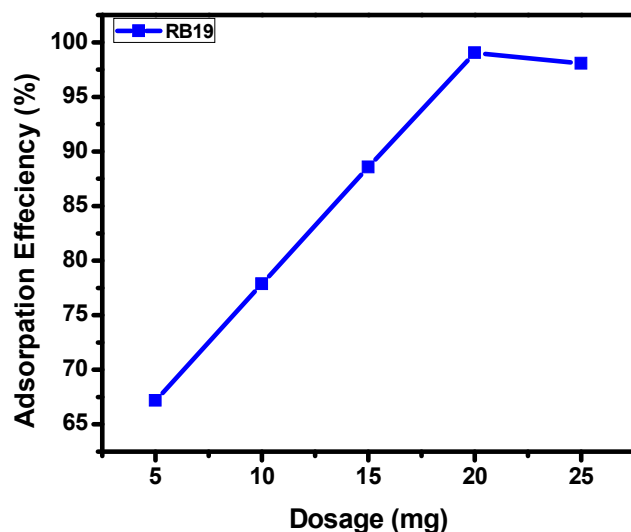
222 The pH of solution is an important parameter to be considered during the adsorption process, as it
 223 can influence the degree of ionization of dye, surface charge of the adsorbent, and also dye molecule
 224 structure .The adsorption of dye RB19 onto zein/nylon nanofiber membrane was studied at different
 225 pH to determine the optimum pH for maximum adsorption as shown in Fig-7. It was found that the
 226 maximum adsorption of RB19 occurred at pH1. When the pH is low, the adsorbent surface becomes
 227 more protonated due to increase in H⁺ concentration, which increase the electrostatic interaction
 228 between the dye anionic (-SO₃⁻) and adsorbent surface (-NH³⁺) resulting more contact between each
 229 other that increase the adsorption efficiency[31]. However increasing the pH cause decrease removal
 230 efficiency, this is due to more negatively charged ions formed that cause deprotonation of amino
 231 groups in zein/nylon nanofibers; as a result adsorbent surface charge turned from highly positive to
 232 highly negative, this causing the electrostatic repulsion between adsorbent surface and dye
 233 solution.

234

**Fig -7** Effect of pH on dye removal by Zein/Nylon nanofiber membrane

244 3.2.3 The effect of adsorbent dosage

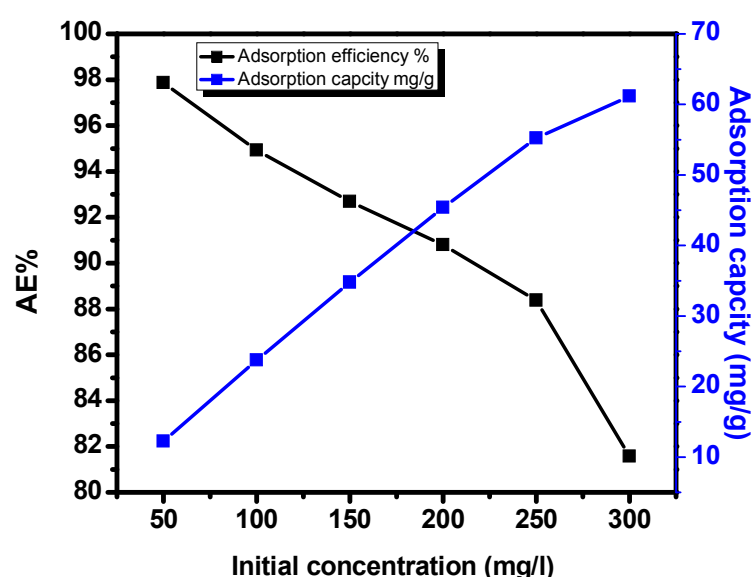
245 The adsorbent dose is an important parameter in adsorption studies which define the removal
 246 efficiency of dye in the given mass of adsorbent. In this study, the removal efficiency of RB19 on the
 247 certain mass of nanofiber was investigated at initial dye concentration of 50mg/l under optimum
 248 conditions of pH and time. Fig-8 shows that the adsorption of RB19 in the acidic medium increased
 249 with the increase in the adsorbent dosage, this is because at higher dosage more binding sites were
 250 available and greater surface area that tended to increase dye adsorption. The maximum adsorption
 251 efficiency of nanofiber was about 98% at 20 mg nanofiber mass at room temperature.
 252
 253



262 Fig-8 Effect of adsorbent dosage on adsorption of RB19

263 3.2.4 The effect of initial dye concentration and Adsorption Isotherms.

264 The adsorption is greatly influenced by the concentration of the analyt . The adsorption of RB19 on
 265 the adsorbent surface of zein/nylon was studied at different initial concentration ranging from
 266 50-300 mg/l at constant temperature and optimum conditions of time, pH and nanofiber mass Fig-9.
 267 The dye adsorption capacities onto adsorbent increased with the increase of the concentration of dye
 268 solutions, the maximum adsorption capacities for RB19 reached 61.2 mg g⁻¹. It was observed that the
 269 removal efficiency of dyes declined slightly with rise in initial dye concentration. This may be due to
 270 more vacant number of active sites and large specific area which was subsequently occupied by the
 271 dye molecule leading to saturation stage and reduction in further removal of RB19 from aqueous
 272 phase.



279

280

281 **Fig-9.** Effect of initial dye concentration on adsorption efficiency of Zein/Nylon-6 nanofibers282 To calculate the adsorption capacity of RB19 on the surface of adsorbent, two well-known
283 adsorption models namely Langmuir and Freundlich [32, 33] isotherm were used respectively to
284 analyze the adsorption isotherms illustrated as:

285
$$\frac{c_e}{q_e} = \frac{1}{b \times q_{\max}} + \frac{c_e}{q_{\max}}$$

286 (4)

287
$$\log q_e = \log k_f + \frac{1}{n} \log c_e$$

288 (5)

289 Where q_{\max} is the maximum adsorption capacity (mg/g), C_e is the equilibrium solution phase
290 concentration, b is related to adsorption free energy and specifies the adsorbent-dye affinity. K_f is291 adsorption capacity and the value $1/n$ from Freundlich isotherm gives information about the relative
292 distribution of active sites; the relative parameter values calculated from the Langmuir and the
293 Freundlich models were listed in Table 2.294 For Langmuir model, q_{\max} which is a measure of monolayer adsorption capacity of the zein/nylon,
295 was calculated 70mg/g for RB19. The values of b were found to be within the range from 0 to 1,
296 indicating that the zein/nylon adsorbent were suitable for Langmuir adsorption for RB19 as shown
297 in Fig-10(a). For Freundlich model, Fig-10(b). The value of n reveals the favorability and degree of
298 heterogeneity. Calculated from Freundlich model, $n > 1$ suggesting favorable adsorption conditions.
299 Based on R^2 value and error analysis, both isotherms favor RB19 adsorptions.

300

301

302 **Table 2. Isotherm parameters for the adsorption of RB19 on Zein/nylon-6 nanofiber at constant**
303 **temperature (25°C).**

DYE

	Langmuir				Freundlich			
	q_{\max} (mg/g)	b (L/g)	R^2	SSE	1/n	K_f (mg/g(L.mg) $^{1/n}$)	R^2	SSE
RB19	70.4	0.114	0.98	0.034	2.32	12.14	0.98	0.032

304

305 The adsorption capacity and other operational parameters of current work were compared with the
306 previously used materials for RB19 (Table 3). It was observed that the Zein/Nylon-6 nanofibers
307 possessed good adsorption capacity. Moreover, the adsorption time achieved from this new

308 Zein/Nylon-6 composite nanofibers for significant dye removal was minimum (i.e. 5 min) that is the
 309 distinctive quality of this adsorbent compared to previously reported materials.

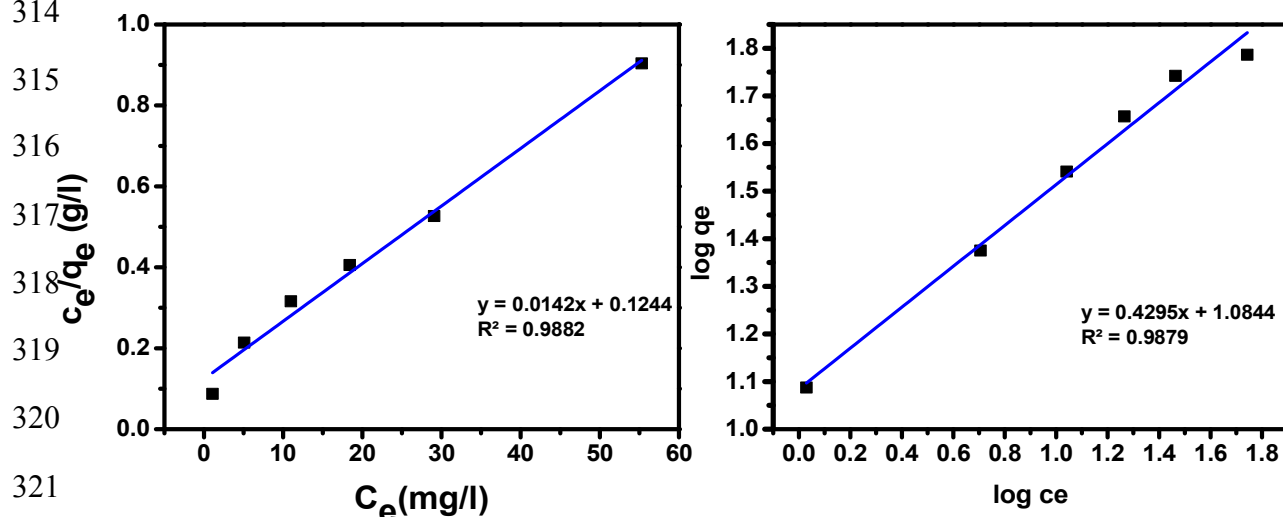
310 **Table 3. Comparison of adsorption capacities and other operational parameters for Reactive blue**
 311 **dyes reported in literature**

312

Dye	Adsorbent	pH	Time (min)	Temperature (K)	Amount (g/L)	Adsorption capacity (mg/g)	Reference
Reactive Blue	Natural ,modified & A.C Wheat straw	6.5	300	R.T	5g	3.2	[35]
RB19	Hollow zein N.P	9.0	1440	294.15	1	1016.0	[18]
RB19	pomegranate seed powder	3	1440	-----	5	9.26	[36]
RB19	Rice straw fly ash	1	60	300	0.9	38.24	[10]
R.B	cashew apple bagasse	2	3500	298.15	10	57.07	[8]
RB19	NiO nanoparticle	3	120	R.T	2.2	98.83	[34]
RB19	magnate/graphene oxide	3	66	R.T	10	62.5	[37]
RB19	grafted chitosan	3	420	-----	0.1g	1498	[38]
Reactive Blue 40	Coal ash	1	900	298.15	100	75.8	[39]
RB19	Zein/nylon-6 nanocomposite	1	5	R.T	70	Present study	

313

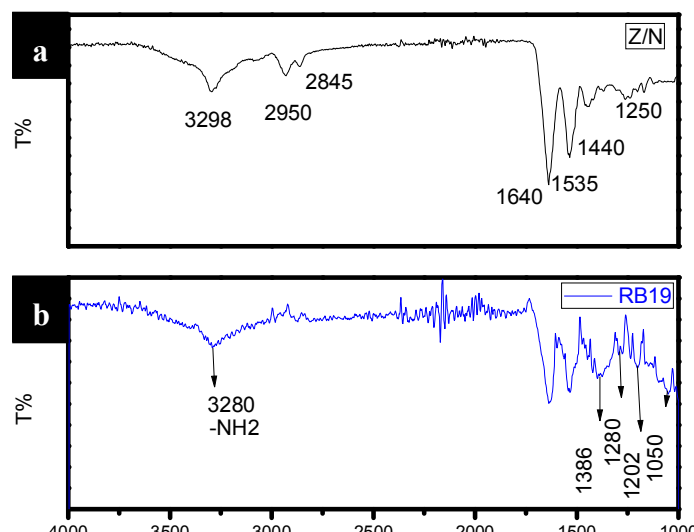
314



321 322 **Fig-10. (a) Langmuir –isotherm (b) Freundlich- isotherm of RB19.**

323 3.3 *The binding mechanism of dye on nanofibers.*

324 Fig-11(a) shows the IR of blended zein/nylon nanofiber, the broad peak at 3298 cm⁻¹ corresponds to
325 (-NH₂ stretching vibration). The stretching at 2950 cm⁻¹ and 2845 cm⁻¹ are related to (-CH)
326 asymmetric and symmetric stretching. The broad/ sharp peaks at 1640 cm⁻¹, 1535 cm⁻¹, 1440 cm⁻¹
327 and 1250 cm⁻¹ were indicative of amide I (C=O stretching vibration), amide II (N-H bending) and
328 amide III (axial deformation vibrations of C-N stretching) respectively. Fig-11(b) show the FTIR
329 analysis after adsorption with RB 19 dye on blended zein/nylon nanofibers, as it can be seen that
330 substantial changes occurred, the new bands at 1050 cm⁻¹ and 1210 cm⁻¹ were the peaks of -SO₃
331 asymmetric stretchings of dye, that confirm the attachment of dye on nanofibers. The peak due to
332 NH₂ stretching also reduced in intensity that suggests that NH₂ group from zein/nylon nanofibers
333 participated in adsorption. Some bands near 1300 cm⁻¹ also overlapped with fresh zein/nylon
334 nanofiber sample that may due to interaction of sulphonate groups of dye with C-N groups of
335 zein/nylon. From the FTIR study, it may be assumed that sulphonate group from dye had
336 preferentially attacked -C-N region of zein/nylon nanofibers. This can be possible either through
337 electrostatic means or by hydrogen bonding from NH group that may have altered C-N stretching
338 also.

347 **Fig-11.** FTIR spectra of zein/nylon nanofibers before (a) and after dye RB19 adsorption (b).

348

349 **4 Conclusion**

350 Efficient and economically viable nanofibers were fabricated via co-electrospinning of two different
351 polymers for RB19 removal from aqueous solution within 10 minutes of adsorption. The acidic pH
352 was favorable for maximum adsorption of anionic dye with the removal efficiency of 94%. The
353 dosage 20mg was sufficient enough to decolorize total dye RB19 at room temperature with
354 adsorption capacity of 70mg/g of nanofiber which is comparatively higher than other well known
355 adsorbents. The binding mechanism between dye and nanofibers is the result of both physical and
356 chemical interactions. The nanofibers are simple, economic with no secondary toxic sludge and
357 minimum waste generation, due to its high surface area and low volume. Another advantage of this
358 nanofiber membrane is its potential application for dye filtration as blending both different
359 polymers yielded nanofiber membrane with excellent mechanical strength.

360 **Acknowledgement**

361 The work was supported by Mehran University of Engineering and Technology Jamshoro, Pakistan
362 and Shinshu University, Japan.

363 References

364 [1] Babu R, Parande AK, Raghu S, and Kumar TP Textile Technology- Cotton Textile Processing: Waste
365 Generation and Effluent Treatment. *The Journal of Cotton Science* (2007)11:141–153.

366 [2] Patil S, Renukdas S, Patel N Removal of methylene blue, a basic dye from aqueous solutions by adsorption
367 using teak tree (*Tectona grandis*) bark powder. *Int. J. Environ. Sci. (2011)* 1: 711–726.

368

369 [3] Brown MA andde vito SC Predicting azo dye toxicity. *Crit. Rev. Environ. Sci. Technol.*, (1993)23 :249.

370

371 [4] Karcher S, Kornmüller A, Jekel M Screeningof commercial sorbents for the removal of reactive dyes. *Dyes*
372 *Pigments*, 51 (2001): 111–125.

373

374 [5] Satheesh R, Vignesh K, Rajarajan M, Sugnathi A, Sreekantan S, Kang M, Kwak B S Removal of congo red
375 from water using quercetin modified Fe₂O₃ nanoparticles as effectivenanoadsorbent. *Mater.Chem.Phys.* (2016),
376 180: 53-65.

377

378 [6] Crini G Non-conventional low-cost adsorbents for dye removal: a review. *Bioresource technology*, (2006), 97:
379 1061-1085.

380 [7]. Alatalo SM, Makila E, Repo E, Heinonen M, Salonen J, Kukk E, Sillanpaa M, Titirici MM. Meso- and
381 microporous soft templated hydrothermal carbons for dye removal from water. *Green Chem.* (2016)18:
382 1137-1146.

383

384 [8] Silva NCG, Souza MCM, Silva Jr. IJ, dos Santos ZM , Rocha MVP Removal of Reactive Turquoise Blue Dye
385 from Aqueous Solution Using a Non-Conventional Natural Adsorbent, *Separation Science and Technology*,
386 (2015) 50: 1616-1628.

387

388 [9] Radae E, Moghaddam MRA, Arami M Removal of reactive blue 19 from aqueous solution by pomegranate
389 residual-based activated carbon: optimization by response surface methodology. *Journal of Environmental*
390 *Health Science & Engineering*, (2014)12:65.

391

392 [10] El-Binary AA, Abd El-Kawi MA, Hafez AM, Rashed IGA, Aboelnaga EE Removal of reactive blue 19 from
393 aqueous solution using rice straw fly ash *J. Mater. Environ. Sci.* (2016) 7 :1023-1036.

394 [11] Tanyildizi MS Modelling of adsorption isotherms and kinetics of reactive dye from aqueous solution by
395 peanut hull. *Chem Eng J.* (2011) 168: 1234-1240

396

397 [12] Zuorroa A, Santarellib MA Lavecchia R Tea Waste: A New Adsorbent for the Removal of Reactive Dyes
398 from Textile Wastewater. *Advanced Materials Research* (2013) 803 : 26-29

399

400 [13] Crini G Non-conventional low-cost adsorbents for dye removal: a review. *Bioresour. Technol.* (2006) 97:
401 1061-1085.

402

403 [14] Batool SS, Imran Z, Hassan S, Rasool K, Ahmad M, Rafiq MA Enhanced adsorptive removal of toxic dyes
404 using SiO₂ nanofibers. *Solid State Sci.* (2016) 55: 13-20.

405

406 [15] Li D, Xia YN Electrospinning of nanofibers: reinventing the wheel? *Adv. Mater.* (2004)16:
407 1151–1170.

408

409 [16] Paraman I, Lamsal BP, Recovery Characterization of zein from corn fermentation coproducts. *Journal of*
410 *Agricultural and Food Chemistry*, (2011)59:3071–3077.

411

412 [17] Alkan D, Aydemir LY, Arcan I, Yavuzdurmaz H, Atabay H I, Ceylan C et al.. Development of flexible
413 antimicrobial packaging materials against *Campylobacter jejuni* by incorporation of gallic acid into zein based
414 films. *Journal of Agricultural and Food Chemistry*, (2011) 59: 11003–11010

415
416 [18] Xu H, Zhang Y, Jiang Q, Reddy N, Yang Y Biodegradable hollow zein nanoparticles for removal of reactive
417 dyes from Wastewater Journal of Environmental Management (2013) 125 : 33-40
418
419 [19] Li X, Song T Fabrication of zein/hyaluronic acid fibrous membranes by electrospinning, Journal of
420 Biomaterials Science, Polymer Edition, (2007) 18:731-742
421
422 [20] McManus MC, Boland ED, Koo HP, Barnes CP, Pawlowski KJ, Wnek GE Mechanical properties of
423 electrospun fibrinogen structures. *Acta Biomater* (2006) 2:19.
424
425 [21] Huang L, Nagapudi K, Apkarian RP, Chaikof EL. Engineered collagen-PEO nanofibers and fabrics. *J*
426 *Biomater Sci Polym Ed* (2001) 12:979.
427
428 [23] Ali S, Khatri Z, Oh K W, Kim IS, Kim S H Zein/Cellulose Acetate Hybrid Nanofibers:Electrospinning and
429 Characterization. *Macromol.Res.* (2014) 22: 971-977.
430
431 [24] Zarrini K, Rahimi A A, Alihosseini F, Fashandi H. Highly efficient dye adsorbent based on
432 polyaniline-coated nylon-6 nanofibers, *J. Clean. Prod.* (2017) 142: 3645-3654.
433 [26] Ma J, Yu F, Zhou L, Jin L, Yang M, Luan J, Tang Y, Fan H, Yuan Z, Chen J Enhanced adsorptive removal of
434 methyl orange and methylene blue from aqueous solution by Alkali activated multiwalled carbon nanotubes,
435 (2012) 4: 5749-5760
436
437 [27] Lagergren S *Kungliga Sevenska Vetenskapsakademiens Handlingar*. (1898) 24: 1-39.
438
439 [28] Ho YS, McKay G Pseudo-second order model for sorption processes. *Process Biochem* (1999) 34: 451-465
440
441 [29] Jr Weber WJ, Morris JC Adsorption Processes for Water Treatment. *J. Sanit. Eng. Div.* (1963) 89:31-60.
442
443 [30] Wang S, Wei JS, Lv Z, Guo F, Jiang Removal of organic dyes in environmental water onto magnetic
444 sulfonic graphene nanocomposite, *CLEAN—Soil, Air, Water* (2013) 41: 992-1001.
445
446 [31] Xu H, Zhang Y, Jiang Q, Reddy N, Yang Y Biodegradable hollow zein nanoparticles for removal of
447 reactive dyes from Wastewater. *J. Environ. Manage.* 2013, 125, 33-40.
448 [32] Langmuir I The constitution and fundamental properties of solids and liquids, *J. Am. Chem. Soc.* (1916)
449 38:2221-2295.
450
451 [33] Freundlich HMF Über die adsorption in lösungen. *Z. Phys. Chem.* (1906) 57: 385-470.
452
453 [34] Khoshhesab ZM & Ahmadi M. Removal of reactive blue 19 from aqueous solutions using NiO
454 nanoparticles: equilibrium and kinetic studies, *Desalination and Water Treatment*, (2016) 57: 20037-20048 DOI:
455 10.1080/19443994.2015.1101713
456
457 [35] Mousa KM, Taha AH Adsorption of Reactive Blue Dye onto Natural and Modified Wheat Straw.
458 *American Journal of Chemical Engineering.* (2016) 4:9-15. doi: 10.11648/j.ajche.20160401.12
459
460 [36] Dehvari M, Ghaneian MT, Ebrahimi A, Jamshidi B, Mootab M Removal of reactive blue 19 dyes from textile
461 wastewater by pomegranate seed powder: Isotherm and kinetic studies. *Int J Env Health Eng* (2016) 5:5.
462
463 [37] Ayazi Z, Khoshhesab ZM, Norouzi S Modeling and optimizing of adsorption removal of Reactive Blue 19
464 on the magnetite/ graphene oxide nanocomposite via response surface methodology, *Desalination and Water*
465 *Treatment* (2016), DOI: 10.1080/19443994.2016.1157705
466
467 [38] Jiang X, Sun Y, Liu L, Wang S, Tian X Adsorption of C.I. Reactive Blue 19 from aqueous solutions by
468 porous particles of the grafted chitosan, *Chemical Engineering Journal* (2014) 235: 151-157.